Combination delivery of two oxime-loaded lipid nanoparticles: Time-dependent additive action for prolonged rat brain protection

Tatiana N. Pashirova, Anissa Braïki, Irina V. Zueva, Konstantin A. Petrov, Vasily M. Babaev, Evgenia A. Burilova, Darya A. Samarkina, Ildar Kh. Rizvanov, Eliana B. Souto, Ludovic Jean, Pierre-Yves Renard, Patrick Masson, Lucia Ya. Zakharova, Oleg G. Sinyashin

PII:	S0168-3659(18)30581-9
DOI:	doi:10.1016/j.jconrel.2018.10.010
Reference:	COREL 9493
To appear in:	*Journal of Controlled Release*
Received date:	15 May 2018
Revised date:	6 October 2018
Accepted date:	8 October 2018

Please cite this article as: Tatiana N. Pashirova, Anissa Braïki, Irina V. Zueva, Konstantin A. Petrov, Vasily M. Babaev, Evgenia A. Burilova, Darya A. Samarkina, Ildar Kh. Rizvanov, Eliana B. Souto, Ludovic Jean, Pierre-Yves Renard, Patrick Masson, Lucia Ya. Zakharova, Oleg G. Sinyashin , Combination delivery of two oxime-loaded lipid nanoparticles: Time-dependent additive action for prolonged rat brain protection. Corel (2018), doi:10.1016/j.jconrel.2018.10.010

Combination delivery of two oxime-loaded lipid nanoparticles: time-dependent additive action for prolonged rat brain protection

Tatiana N. Pashirova[a*], Anissa Braïki[b], Irina V. Zueva[a], Konstantin A. Petrov[a,c], Vasily M. Babaev[a], Evgenia A. Burilova[a,c], Darya A. Samarkina[a], Ildar Kh. Rizvanov[a], Eliana B. Souto[d,e], Ludovic Jean[b], Pierre-Yves Renard[b], Patrick Masson[c], Lucia Ya. Zakharova[a*], Oleg G. Sinyashin[a]

[a]*Arbuzov Institute of Organic and Physical Chemistry, FRC Kazan Scientific Center of RAS, Arbuzov St., 8, Kazan, 420088, Russia*

[b]*Normandie Univ, UNIROUEN, INSA Rouen, CNRS, COBRA (UMR 6014), Rouen, France*

[c]*Kazan Federal University, Kremlyovskaya St., 18, Kazan, 420008, Russia*

[d]*Department of Pharmaceutical Technology, Faculty of Pharmacy, University of Coimbra, Coimbra, Portugal*

[e]*REQUIMTE/LAQV, Group of Pharmaceutical Technology, Faculty of Pharmacy, University of Coimbra, Coimbra, Portugal*

Corresponding Authors

Tatiana N. Pashirova, Arbuzov Institute of Organic and Physical Chemistry, FRC Kazan Scientific Center of RAS, Arbuzov str. 8, Kazan, 420088, Russian Federation, tel: (007) 843 273 22 93, fax: (007) 843 273 22 53, E-mail: tatyana_pashirova@mail.ru

Lucia Ya. Zakharova, Arbuzov Institute of Organic and Physical Chemistry, FRC Kazan Scientific Center of RAS, Arbuzov St. 8, Kazan, 420088, Russian Federation, tel: (007) 843 273 22 93, fax: (007) 843 273 22 53, E-mail: lucia@iopc.ru

ABSTRACT

A novel approach for brain protection against poisoning by organophosphorus agents is developed based on the combination treatment of dual delivery of two oximes. Pralidoxime chloride (2-PAM) and a novel reactivator, 6-(5-(6,7-dimethoxy-3,4-dihydroisoquinolin-2(1H)-yl)pentyl)-3-hydroxy picolinaldehyde oxime (3-HPA), have been loaded in solid-lipid nanoparticles (SLNs) to offer distinct release profile and systemic half-life for both oximes. To increase the therapeutic time window of both oximes, SLNs with two different compartments were designed to load each respective drug. Oxime-loaded SLNs of hydrodynamic diameter between 100 and 160 nm and negative zeta potential (-30 to -25 mV) were stable for a period of 10 months at 4 ºC. SLNs displayed longer circulation time in the bloodstream compared to free 3-HPA and free 2-PAM. Oxime-loaded SLNs were suitable for intravenous (*iv*) administration. Paraoxon-poisoned rats ($0.8\times LD_{50}$) were treated with 3-HPA-loaded SLNs and 2-PAM+3-HPA-loaded SLNs at the dose of 3-HPA and 2-PAM of 5 mg/kg. Brain AChE reactivation up to 30% was slowly achieved in 5 hours after administration of 3-HPA-SLNs. For combination therapy with two oximes, a time-dependent additivity and increased reactivation up to 35% were observed.

Keywords: Solid-Lipid Nanoparticles, Blood-brain barrier, Acetylcholinesterase, Organophosphorus agent, Oxime, Paraoxon.

1. Introduction

Multidrug combination therapy is one of the promising approaches for treatment of chronic diseases. Nanotechnological "two-in-one" approach using nanoparticles for packaging multiple drugs in single carriers allows the improvement of drugs' bioavailability, with the simultaneous decrease of administered doses and adverse side-reactions [1-4]. Nanoparticles exhibit targeted delivery of drugs and modified release profile and, when loaded with two drugs, may foster synergistic therapeutic outcomes [2]. To date, prevention of irreversible brain damages after acute organophosphorus (OP) poisoning is still a difficult problem, in particular in case of delayed medical care [5]. OP threat has become increasingly important due to acts of terrorism around the globe that have increased markedly in recent decades, and due to the proved use of these agents against civilian populations in Iraq and Syria. The acute toxicity of OPs results from covalent inhibition, phosphylation, of acetylcholinesterase (AChE). Low OP doses do not induce clinical manifestations of cholinergic impairment. It is accepted that clinical signs of poisoning appear when cholinesterase activity drops below 50% [6]. Severe signs, in particular convulsions, appear when AChE activity of poisoned patients is below 10-20% [7]. In humans, brain AChE activity less than 10% is associated with respiratory failure and death [8]. Thus, the current emergency treatment of acute OP poisoning consists in administering a combination of AChE reactivator (quaternary oximes), atropine as anticholinergic drug to protect muscarinic receptors, and an anticonvulsant to prevent irreversible brain damage [5,9]. However, current quaternary oximes are unable to reactivate phosphylated AChE in the central nervous system (CNS) because they do not cross significantly the blood-brain barrier (BBB) [10]. Combination of two oximes has been shown to improve the emergency treatment of OP poisoning by covering a wide spectrum of organophosphorus agents [11-13]. Moreover, association of two oximes revealed a beneficial effect by broadening the spectrum of the individual oximes [12].

Nanoparticles as oxime delivery vehicles are therefore promising for this purpose [14,15]. Recently, our group showed that 2-PAM-loaded solid lipid nanoparticles are able to protect against paraoxon central toxicity [16]. Other researchers have also been working in that direction [14]. However, due to rapid elimination of 2-PAM, the percentage of reactivation of central AChE of the brain was low. To realize the potential of combination therapy at the present study, design of formulations for delivery of two oximes with different physiochemical properties has been investigated, in particular, the water-soluble charged oxime pralidoxime chloride (2-PAM) and a poorly water soluble new uncharged hydrophobic oxime 6-(5-(6,7-Dimethoxy-3,4-dihydroisoquinolin-2(1H)-yl)pentyl)-3-hydroxy picolinaldehyde oxime (3-HPA) were combined.

3-HPA displays a key 3-hydroxy-2-pyridine aldoxime structure as the reactivator moiety linked to a dimethoxy dihydroisoquinolin as the AChE peripheral site binder in order to increase its affinity for phosphylated enzyme. See Fig. 1 for structure of 3-HPA. 3-HPA showed an exceptional potential for reactivation of VX-, paraoxon-, and tabun-phosphylated AChE [17].

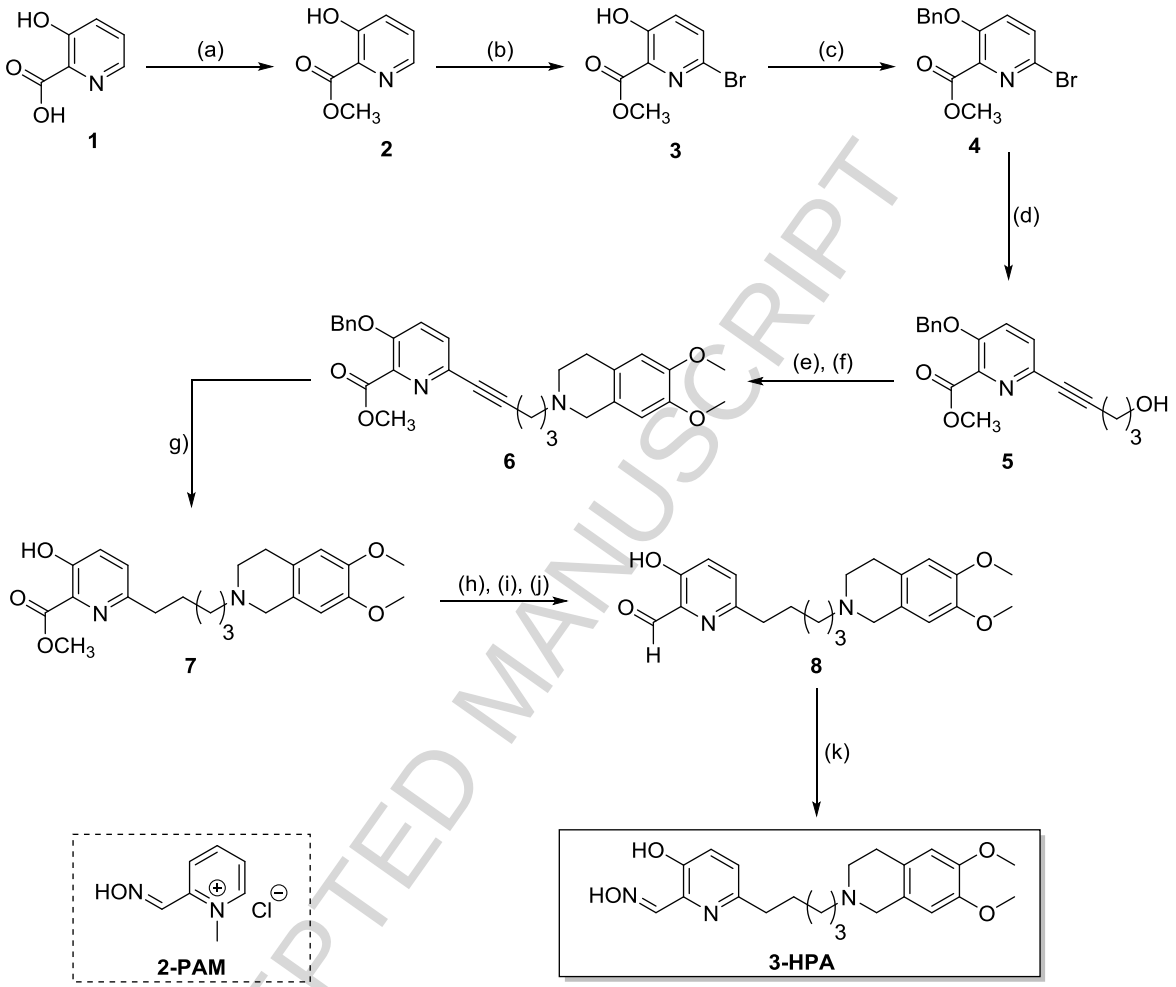

(a) H_2SO_4, MeOH, reflux, 6h, 99%; (b) Br_2, H_2O, ice, 0°C, 1-2h, 99%; (c) BnBr, K_2CO_3, acetone, reflux, 12 h, 95%; (d) 4-pentyn-1-ol, $Pd(PPh_3)_4$, CuI, NEt_3/CH_2Cl_2 (1:1, v/v), rt, 12 h, 96%; (e) MsCl, NEt_3, CH_2Cl_2, rt, 2 h, 99%.; (f) TIQ.HCl, K_2CO_3, CH_3CN, reflux, 12 h, 74%; (g) H_2 (1 atm), $Pd(OH)_2$, MeOH, rt, 12 h, 99%.; (h), TBDMSOTf, NEt_3, CH_2Cl_2, rt, 2 h; (i) DIBAL-H, CH_2Cl_2, -78°C, 15 min; (j) TBAF, THF, 0 °C, 30 min, 67% over 3 steps; (k) AcONa, $NH_2OH.HCl$, MeOH, rt, 3-4 h, 73%.

Fig. 1. Structure of the oximes and synthetic route of hydrophobic oxime 6-(5-(6,7-Dimethoxy-3,4-dihydroisoquinolin-2(1H)-yl)pentyl)-3-hydroxy picolinaldehyde oxime (3-HPA).

Owing to the difficulty to reactivate cholinesterases inhibited by phosphoramidates such as tabun as the prototype, 3-HPA constitutes a real *progress* in medical countermeasures of OP poisoning. For this purpose, biocompatible and biodegradable solid-lipid nanoparticles (SLNs) [18,19], prepared by the double emulsion method [20] with two different compartments to incorporate both oximes with different release times, are appropriate. These encapsulated oximes would be

suitable for intravenous (*i.v.*) administration, and *in vivo* efficient therapy of rats poisoned by paraoxon. Here we have extended our previous work [16] and pursued several tasks that remain to be solved: i) overcoming BBB for 2-PAM and its reactivating action of brain AChE; ii) increasing the bioavailability of the novel oxime 3-HPA; iii) achieving sequential release of both oximes and expanding the time window of oxime therapy.

2. Materials and methods

2.1. Chemicals

DYNASAN® 114 (Trimyristin) triglycerides was a gift from CREMER OLEO GmbH & Co. KG (Hamburg, Germany), Lipoid® S75, 75% soybean phosphatidylcholine was a gift from Lipoid GmbH (Ludwigshafen, Germany), Tween® 80 (Polysorbate 80) (BioXtra, Sigma-Aldrich, product of France), Glycerol (≥ 99.5 %, Sigma-Aldrich ChemieGmbh, Steinheim, Germany), Pyridine-2-aldoxime methochloride (2-PAM chloride, Pralidoxime chloride) (≥ 97 %, Sigma-Aldrich), Dichloromethane for HPLC (PanReac AppliChem GmbH, Darmstadt, Germany), Ultra-purified water (18.2 MΩcm resistivity at 25°C) was produced from Direct-Q 5 UV equipment (Millipore S.A.S. 67120 Molsheim-France). Solvents were purified by a dry solvent station MB-SPS-800 (MBraun) immediately prior to use. Triethylamine was distilled from CaH_2 and stored over BaO or KOH. All reagents were obtained from commercial suppliers (Sigma Aldrich, Acros, TCI) unless otherwise stated.

2.2. Synthesis of 3-HPA

Column chromatography purifications were performed on silica gel (40–63 µm) from Macherey-Nagel. Thin-layer chromatography (TLC) was carried out on Merck DC Kieselgel 60 F-254 aluminium sheets. Compounds were visualized by UV irradiation and/or spraying with a stain solution (KMnO4, ninhydrin or 2,4-DNP), followed by charring at 150 °C. ^{1}H and ^{13}C NMR spectra were recorded with a Bruker DPX 300 spectrometer (Bruker, Wissembourg, France). Chemical shifts are expressed in parts per million (ppm) from $CDCl_3$ (δ_H = 7.26 ppm, δ_C = 77.16 ppm). *J* values are expressed in Hz. Mass spectra were obtained with a Finnigan LCQ Advantage MAX (ion trap) apparatus equipped with an electrospray source. High-resolution mass spectra were obtained with a Varian MAT 311 spectrometer using electrospray analysis. Analytical HPLC was performed on a Thermo Electron Surveyor instrument equipped with a PDA detector under the following conditions: Thermo Hypersil GOLD C18 column (5 µm, 4.6 x 100 mm) with CH_3CN and 0.1% aq. trifluoroacetic acid (TFA) as eluents [0.1% aq. TFA/ CH_3CN (100/0)

(5 min), followed by linear gradient from 0% to 100% of CH_3CN (45 min), then 100% CH_3CN (10 min)], at a flow rate of 1.0 mL/min and *UV detection Max Plot* 220−360 nm.

Synthesis of Methyl 3-hydroxypicolinate (Compound 2). To a suspension of 3-hydroxypicolinic acid **1** (10 g, 72 mmol, 1 equiv) in methanol (150 mL, 0.5 M) was added dropwise at 0 °C a concentrated sulfuric acid (12 mL, 216 mmol, 3 equiv.). The obtained solution was stirred at reflux 6 h. The cooled reaction mixture was concentrated under reduced pressure. The pH was adjusted at 8.5 with an aqueous solution of saturated $NaHCO_3$ and solid $NaHCO_3$. The aqueous layer was extracted with EtOAc and the combined organic layer was washed with brine, dried over $MgSO_4$ and concentrated under reduced pressure to give **2** as a white solid (10.9 g, 99%). *Rf* =0.3 (Petroleum ether/EtOAc 1/1, v/v). m.p. = 74 °C. ^{1}H NMR (300 MHz, $CDCl_3$): δ (ppm) = 4.06 (s, 3H), 7.34 (dd, *J* = 3.9, 8.4 Hz, 1H), 7.38 (dd, *J* = 1.5, 8.4 Hz, 1H), 8.38 (dd, *J* = 1.5, 3.9 Hz, 1H), 10.64 (s, 1H). ^{13}C NMR (75 MHz, $CDCl_3$): δ = 53.2, 126.3, 129.8, 130.2, 141.6, 158.9, 169.9. MS (ESI+): *m/z* (%): 154 (100) $[M+H]^+$.

Synthesis of Methyl 3-hydroxy-6-bromopicolinate (Compound 3). To a solution of methyl 3-hydroxypicolinate **2** (10 g, 65.36 mmol) in osmosed water (0.1 M) with crushed ice at 0 °C, was added portionwise bromine (4 x 1.02 mL every 30 min, 78.4 mmol, 1.2 equiv) under vigorous stirring. The mixture was vigorously stirred at 0 °C for 1-2 h. The solution was extracted by dichloromethane and the combined organic layers were washed with brine, dried over $MgSO_4$ and concentrated under reduced pressure to give **3** as a white-off solid (15.08 g, 99%). *Rf* = 0.3 (Petroleum ether/EtOAc 3/2, v/v). ^{1}H NMR (300 MHz, $CDCl_3$) δ (ppm) = 4.07 (s, 3H), 7.29 (d, *J* = 8.7 Hz, 1H), 7.58 (dd, *J* = 0.3, 8.7 Hz, 1H), 10.72 (br s, 1H). ^{13}C NMR (75 MHz, $CDCl_3$) δ (ppm) = 53.5, 129.5, 130.0, 130.7, 134.5, 158.5, 169.1. MS (ESI+): *m/z* (%): 234 (85) and 232 (100) $[M+H]^+$.

Synthesis of Methyl 3-(benzyloxy)-6-bromopicolinate (Compound 4). To a solution of methyl 3-hydroxy-6-bromopicolinate **3** (11.6 g, 49.8 mmol), in acetone (200 mL, 0.25 M) was added successively K_2CO_3 (21 g, 149 mmol, 3 equiv) and benzyl bromide (12 mL, 100 mmol, 2.0 equiv). The heterogeneous reaction mixture was reflux overnight. Salts were removed by filtration and the crude product was concentrated under reduced pressure. Purification by flash chromatography (Petroleum ether/EtOAc 95/5 to 3/2, v/v) afforded the desired product **4** as a white solid (15.2 g, 95%). *Rf* = 0.4 (Petroleum ether/EtOAc 8/2, v/v). ^{1}H NMR (300 MHz, $CDCl_3$): δ (ppm) = 3.97 (s, 3H), 5.21 (s, 2H), 7.24 (d, *J* = 8.7 Hz, 1H), 7.47-7.34 (m, 5H), 7.51 (d, *J* = 8.7 Hz, 1H). ^{13}C NMR (75 MHz, $CDCl_3$): δ (ppm) = 52.9, 71.2, 125.0, 126.9, 128.4, 128.8, 131.2, 131.4, 135.2, 139.8, 154.0, 164.0. MS (ESI+): *m/z* (%): 324 (85) and 322 (100) $[M+H]^+$.

Synthesis of Methyl 3-(benzyloxy)-6-(5-hydroxypent-1-ynyl)picolinate (Compound 5). To a solution of methyl 3-(benzyloxy)-6-bromopicolinate **4** (3.19 g, 9.90 mmol) in dichloromethane (66 mL) and triethylamine (33 mL) was added 4-pentyn-1-ol (650 µL, 9.93 mmol, 1 equiv). The resulting mixture was degassed for 20 min with argon. CuI (200 mg, 1.02 mmol, 0.1 equiv.) and $Pd(PPh_3)_4$ (527 mg, 0.50 mmol, 0.05 equiv.) were then poured and the solution was stirred under argon at room temperature overnight. The reaction mixture was concentrated under reduced pressure. Purification by flash chromatography (Petroleum ether/EtOAc 7/3 to 3/7, v/v) afforded the desired product **5** as a yellow oil that crystallized upon standing (3.1 g, 96%). *Rf* = 0.33 (Petroleum ether/EtOAc 3/7, v/v). ^{1}H NMR (300 MHz, $CDCl_3$) δ (ppm) = 1.86 (qt, *J* = 6.4 Hz, 2H), 2.38 (br s, 1H), 2.54 (t, *J* = 7.0 Hz, 2H), 3.78 (t, *J* = 6.2 Hz, 2H), 3.96 (s, 3H), 5.20 (s, 2H), 7.30-7.45 (m, 7H). ^{13}C NMR (75 MHz, $CDCl_3$) δ (ppm) = 15.9, 31.0, 52.7, 61.4, 70.9, 79.6, 89.8, 121.9, 127.0, 128.3, 128.8, 130.1, 135.4, 135.6, 140.0, 153.0, 164.9. MS (ESI+): *m/z* (%): 673 (100) $[2M + Na]^+$, 348 (95) $[M+Na]^+$ and 326 (100) $[M+H]^+$.

Synthesis of Methyl 3-(benzyloxy)-6-(5-(6,7-dimethoxy-3,4-dihydroisoquinolin-2(1*H*)-yl)pent-1-yn-1-yl)picolinate (Compound 6). Methanesulfonyl chloride (1.6 mL, 20.45 mmol, 1.5 equiv.) was added dropwise to a solution of methyl 3-(benzyloxy)-6-(5-hydroxypent-1-ynyl)picolinate **5** (4.73 mg, 13.63 mmol) and triethylamine (5.6 mL, 40.89 mmol, 3 equiv) in dry dichloromethane (0.1 M) at 0 °C. The solution was stirred room temperature for 2 h, washed with brine, dried under $MgSO_4$ and concentrated under reduced pressure. To a solution of the crude product in dry CH_3CN (0.1 M) were added 6,7-dimethoxy-1,2,3,4-tetrahydroisoquinoline hydrochloride (TIQ.HCl, 2.1 g, 1.5 equiv.) and K_2CO_3 (3.4 g, 3 equiv.). The mixture was refluxed overnight. The crude mixture was filtered, concentrated under reduced pressure and purified by flash chromatography on silica gel (CH_2Cl_2/MeOH, 100/0 to 95:5, v/v) to give the desired product **6** (2.86 g, 74%) as an orangeous oil. R_f = 0.2 (CH_2Cl_2/MeOH 95/5). ^{1}H NMR (300 MHz, $CDCl_3$) δ (ppm) = 1.93 (qt, *J* = 6.9 Hz, 2H), 2.51 (t, *J* = 6.9 Hz, 2H), 2.63 (t, *J* = 6.9 Hz, 2H), 2.72 (t, *J* = 5.4 Hz, 2H), 2.83 (t, *J* = 5.4 Hz, 2H), 3.57 (s, 2H), 3.83 (s, 3H), 3.84 (s, 3H), 3.96 (s, 3H), 5.19 (s, 2H), 6.53 (s, 1H), 6.60 (s, 1H), 7.25–7.45 (m, 7H).^{13}C NMR (75 MHz, $CDCl_3$) δ (ppm) = 17.4, 26.0, 28.7, 51.0, 52.7, 55.7, 55.8, 55.9, 57.2, 70.7, 79.5, 90.1, 109.4, 112.3, 121.7, 126.2, 126.6, 126.9, 128.2, 128.7, 130.0, 135.4, 135.5, 139.9, 147.1, 147.4, 152.9, 164.8. MS (ESI^+): *m/z* (%): 501 (100) $[M+H]^+$.

Synthesis of Methyl 6-(5-(6,7-dimethoxy-3,4-dihydroisoquinolin-2(1*H*)-yl)pentyl)-3-hydroxypicolinate (Compound 7). To a solution of **6** (2.5 g, 5 mmol) in degassed methanol (0.05 M) was added Pearlman's catalyst (500 mg, 20% Pd, moisture 50%). The solution was bubbled with H_2 and the reaction was stirred overnight at room temperature under H_2 atmosphere

(1 atm). The mixture was filtrated through celite and concentrated under reduced pressure to give the desired product **7** as a orangeous oil that crystallized upon standing (2.07 g, 99%). ^{1}H NMR (300 MHz, $CDCl_3$) δ (ppm) = 10.59 (s, 1H), 7.30 (br s, 1H), 7.26 (s, 1H), 6.58 (s, 1H), 6.51 (s, 1H), 4.04 (s, 3H), 3.84 (s, 3H), 3.83 (s, 3H), 3.53 (s, 2H), 2.87 – 2.74 (m, 4H), 2.68 (t, *J* = 5.7 Hz, 2H), 2.55 – 2.42 (m, 2H), 1.67 (m, 4H), 1.53 – 1.35 (m, 2H). ^{13}C NMR (75 MHz, $CDCl_3$) δ (ppm) = 169.8, 156.9, 153.6, 147.7, 147.3, 129.0, 128.5, 126.4, 124.9, 111.1, 109.2, 56.9, 55.7, 55.6, 54.4, 52.9, 50.1, 37.2, 29.6, 27.0, 26.8, 25.9. MS (ESI^+): *m/z* (%): 415 (100) $[M+H]^+$.

Synthesis of 6-(5-(6,7-Dimethoxy-3,4-dihydroisoquinolin-2(1*H*)-yl)pentyl)-3-hydroxypicolinaldehyde (Compound 8). To an ice-bath cooled solution of methyl 6-(5-(6,7-dimethoxy-3,4-dihydroisoquinolin-2(1*H*)-yl)pentyl)-3-hydroxypicolinate **7** (2.07 g, 5.0 mmol, 1 equiv) in dry dichloromethane (0.05 M) were successively added dry triethylamine (1.6 mL, 11 mmol, 2.2 equiv.) and *tert*-butyldimethylsilyl trifluoromethanesulfonate (1.3 mL, 5.5 mmol, 1.1 equiv.). The mixture was stirred at room temperature for 2 h under argon atmosphere. The organic layer was washed with brine, dried over $MgSO_4$ and concentrated under reduced pressure. To a solution of the resulting residue in dry dichloromethane (0.05 M) at -78 °C, was added dropwise DIBAL-H (12.5 mL, 1 M in dichloromethane, 12.5 mmol, 2.5 equiv.). Then, the reaction mixture was stirred at this temperature for 15 min. The reaction was quenched with methanol (12.5 mL) and the mixture was allowed to warm at room temperature. The organic layer was washed with an aqueous solution of NaOH (1 M), dried over $MgSO_4$ and concentrated under reduced pressure. Then, tetrabutylammonium fluoride (5.5 mL, 1.1 equiv., 1 M in THF) was added at 0 °C to the residue in dry THF (0.1 M) and the mixture was stirred for 30 min at 0-5 °C. After concentration under reduced pressure, a purification by flash chromatography on silica gel (CH_2Cl_2/MeOH 100:0 to 95:5, v/v) afforded **8** (1.29 g, 67%) as a yellow oil. *Rf* = 0.27 (CH_2Cl_2/MeOH, 95 :5). ^{1}H NMR (300 MHz, $CDCl_3$) δ = 10.03 (br s, 2H), 7.31 (d, *J* = 8.7 Hz, 1H), 7.27 (d, *J* = 8.7 Hz, 1H), 6.60 (s, 1H), 6.53 (s, 1H), 3.84 (d, *J* = 1.6 Hz, 6H), 3.59 (s, 2H), 2.95 – 2.67 (m, 6H), 2.63 – 2.41 (m, 2H), 1.90 – 1.57 (m, 4H), 1.46 (d, *J* = 7.0 Hz, 2H). ^{13}C NMR (75 MHz, $CDCl_3$) δ = 198.5, 156.8, 154.7, 147.4, 147.1, 135.6, 129.6, 126.2, 126.1, 125.9, 111.2, 109.4, 77.1, 57.9, 55.8, 55.7, 55.5, 50.7, 37.1, 29.5, 28.3, 27.0, 26.8. MS (ESI^+): *m/z* (%): 385 (100) $[M+H]^+$.

Synthesis of 6-(5-(6,7-dimethoxy-3,4-dihydroisoquinolin-2(1*H*)-yl)pentyl)-3-hydroxy-2-pyridine aldoxime (3-HPA). To a solution of aldehyde **8** (1.29 g, 3.35 mmol) in methanol (stored on MS 3 Å, under argon, 0.1 M) were added successively $NH_2OH.HCl$ (245 mg, 3.52 mmol, 1.05 equiv.) and sodium acetate (305 mg, 3.68 mmol, 1.1 equiv.). The mixture was stirred at room temperature under argon atmosphere until completion (3-4 h). After concentration under

reduced pressure, the residue was purified by flash chromatography on silica gel (gradient CH_2Cl_2/MeOH, 98 :2 to 90 :10) to give the desired oxime **3-HPA** as a white solid (976 mg, 73%). *Rf* = 0.2 (CH_2Cl_2/MeOH 95:5). ^{1}H NMR (300 MHz, $CDCl_3$) δ (ppm) = 1.33–1.43 (m, 2H), 1.55–1.73 (m, 4H), 2.55–2.72 (m, 2H), 2.85–2.96 (m, 4H), 3.74 (s, 1H), 3.81 (s, 3H), 3.82 (s, 3H), 6.51 (s, 1H), 6.58 (s, 1H), 6.95 (d, *J* = 8.4 Hz, 2H), 7.10 (d, *J* = 8.4 Hz, 2H), 8.28 (s, 1H), 9.88 (br s, 1H). ^{13}C NMR (75 MHz, $CDCl_3$) δ (ppm) = 14.2, 22.7, 26.1, 26.9, 37.1, 50.3, 54.7, 55.8, 55.9, 57.3, 76.6, 109.3, 111.2, 123.8, 124.3, 125.1, 135.1, 147.5, 147.8, 152.4, 153.7, 160.6, 171.9. MS (ESI+): *m/z* (%): 400 (100) $[M+H]^+$. HRMS (ESI^+): *m/z* calcd for $C_{22}H_{30}N_3O_4$ 400.2236; found: 400.2230. HPLC: t_R = 19.15 min (purity = 97.83%).

2.3. Preparation of 3-HPA-loaded SLNs and 2-PAM+3-HPA-loaded SLNs

The multiple emulsion (w/o/w) method described by Pashirova et al [13] was chosen for preparing SLNs. The hydrophobic oxime 3-HPA (0.04 g) was melted in the lipid phase composed of lipid (Dynasan 114), 5 mL glycerol and Lipoid® S75. Temperature was 5-10°C above the melting point of lipid. Then the aqueous phase (1 ml) was added to the lipid phase composed of lipid (Dynasan 114), 5 mL glycerol, Lipoid® S75 and the hydrophobic oxime 3-HPA (0.04 g) at the same temperature and homogenized with high shear homogenizer (Ultra-Turrax®, IKA, T18, Germany) for 10 minutes, under stirring intensity of 10,000 rpm. The mixture was kept at constant temperature during homogenization. Then, this w/o emulsion was poured into a total weight (40g) of cooled solutions of surfactant (Tween® 80) under magnetic stirring (750 rpm) (Heidolph, Germany) for 20 min to allow the formation of SLNs. Briefly, for production of SLNs loading two oximes (hydrophilic oxime (2-PAM) and hydrophobic oxime 3-HPA) the same method was used by replacing the inner aqueous phase (1 ml), which was prepared by dissolving 2-PAM (0.04 g) in ultra-purified water. Dynasan 114 was selected as the solid lipid and Tween 80 as surfactant added to the external aqueous phase of the multiple emulsion.

2.4. Characterization of SLNs

The mean particle size, zeta potential and polydispersity index of SLNs were determined by dynamic light scattering (DLS) measurements, using the Malvern Instrument Zetasizer Nano (Worcestershire, UK). The measured autocorrelation functions were analyzed by Malvern DTS software, applying the second-order cumulant expansion methods. The effective hydrodynamic radius (R_H) was calculated according to the Einstein-Stokes equation $D=k_BT/6\pi\eta R_H$, in which D

is the diffusion coefficient, k_B the Boltzmann's constant, T the absolute temperature, and η the viscosity. The diffusion coefficient was measured at least in triplicate for each sample. The average error of measurements was approximately 4%. All samples were diluted with ultra-purified water to suitable concentration and analyzed in triplicate.

2.5. Encapsulation efficiency and loading capacity

Encapsulation efficiency (*EE*, %) and loading capacity (*LC*, %) were assessed for samples containing 2-PAM. These parameters were determined indirectly by filtration/centrifugation technique, measuring free 2-PAM (non-encapsulated) by spectrophotometry. A volume of 0.5 mL of each 2-PAM+3-HPA-loaded SLNs was placed in centrifugal filter devices Ultracel 100K (100,000 MWCO, Amicon Millipore Corporation, Bedford, Massachusetts) to separate lipid and aqueous phases and centrifuged at 10,000 rpm, for 15 minutes (Eppendorf AG, Hamburg, Germany). Free 2-PAM was quantified by measuring the absorbance using a Specord 250 Plus (Analytik Jena AG, Germany) at 294 nm (the molar extinction coefficient of 2-PAM at 294 nm is 11962 $M^{-1}{\cdot}cm^{-1}$ at pH = 7.4). Encapsulation efficiency (*EE*, %) and loading capacity (*LC*, %) were assessed for samples containing 3-HPA. These parameters were determined indirectly by centrifugation technique, measuring free 3-HPA (non-encapsulated) by spectrophotometry. A volume of 1 mL of each 3-HPA-loaded SLNs or 2-PAM+3-HPA-loaded SLNs were placed in 2 mL Eppendorf tube and was centrifuged (Eppendorf AG, Hamburg, Germany) for 10 min at 5000 rpm to remove precipitated free 3-HPA compound. A volume of 0.2 mL of each 3-HPA-loaded SLNs was placed in new 2 mL Eppendorf tube and 1mL of dichloromethane was added to each sample. Then extraction of 3-HPA was performed, using the Vortex shaker (Neutec F202A0176 Model ZX3 Advanced Vortex Mixer) at 4000 rpm for 10 min. The mixture (~1.2 mL) was centrifuged (Eppendorf AG, Hamburg, Germany) for 6 min at 5000 rpm to separate the layers. The lower organic layer was transferred to a flask and evaporated to dryness under a gentle stream of nitrogen. 3-HPA extraction procedure was repeated 2 times. The residue was then reconstituted with 3 mL of dichloromethane. Loaded 3-HPA was quantified by UV absorbance using a Specord 250 Plus (Analytik Jena AG, Germany) at 315 nm (the extinction coefficient of 3-HPA at 315 nm is 8686 $M^{-1}{\cdot}cm^{-1}$ (Fig. 1S, SM). The parameters were calculated against appropriate calibration curve, using the following equation [21]:

$$EE(\%) = \frac{Total\ amount\ of\ oxime - Free\ oxime}{Total\ amount\ of\ oxime} \times 100\% \qquad (1)$$

$$LC(\%) = \frac{Total\ amount\ of\ oxime - Free\ oxime}{Total\ amount\ of\ lipid} \times 100\% \quad (2)$$

2.6. In vitro 2-PAM or 3-HPA release profile

The release of 2-PAM or 3-HPA from SLNs was performed using the dialysis bag diffusion method. The dialysis bags retain SLNs and allow released 2-PAM or 3-HPA to diffuse into the medium. The bags were soaked in Milli-Q water for 12 h before use. 5 milliliters of SLNs were poured into the dialysis bag and the two ends of the bag were sealed with clamps. 50 mL methanol and 50 mL of 0.025 M sodium phosphate buffer pH 7.4were used as the receiving phase. The vessel was placed in a thermostatic shaker (New Brunswick, USA), at 37ºC, under a stirring rate of 150 rpm. At predetermined time intervals, 1 mL samples were withdrawn, and analyzed by determining the absorbance at 294 nm for 2-PAM and at 315 nm for 3-HPA (Fig. 2S, SM) using a Specord 250 Plus (Analytik Jena AG, Germany) and HPLC-MS. At predetermined time intervals, 10 μL of samples were diluted in methanol and water (70:30, v/v). Details of HPLC-MS analysis are described below (in section 2.8). Calibration curve of 3-HPA in sodium phosphate buffer (0.025 M) is given in Fig 3S. All samples were analyzed in triplicate.

2.7. Pharmacokinetic and tissue distribution study

All experiments involving animals were performed in accordance with the guidelines set forth by the European Communities Council Directive of November 24, 1986 (86/609/EEC) and the protocol of experiments approved by the Animal Care and Use Committee of Kazan Federal University.

Wistar rats of both sexes were purchased from the Laboratory Animal Breeding Facility (Branch of Shemyakin-Ovchinnikov Institute of Bioorganic Chemistry, Puschino, Moscow Region, Russia) and were allowed to acclimate to their environment in the vivarium for at least 1 week before experiments. Animals were kept in sawdust-lined plastic cages in a well-ventilated room at 20–22 °C in a 12-h light/dark cycle, 60−70% relative humidity and given *ad libitum* access to food and water.

The maximum recommended volume for *i.v.* administration into rats is 1-2 ml [22]. Proceeding from this maximum recommended volume, the dose of 5 mg/kg 2-PAM and/or 5 mg/kg 3-HPA was selected. Sample was slowly administered into the tail vein of rats weighing 200-250g.

Two groups of animals were set: 3-HPA solution (DMSO-water (50 w/w) or 3-HPA-SLNs or 2-PAM+3-HPA-SLNs, respectively at a dose of 5 mg/kg (~ 1 ml 0.1% w/w of 3-HPA) were

injected in the tail vein of each group. At predetermined time intervals (5, 15, 30, 45, 60, 120, 180, 240 and 300 min after injection), five rats at each time point from each group were deeply anesthetized by isoflurane inhalation until the tail-pinch reflex disappeared, and blood samples (1ml) were collected, placed into heparinized test tubes and centrifuged (at 12,000 rpm, 10 min, 4ºC) to get plasma. Thereafter, animals were quickly decapitated and tissue samples (whole brain) were immediately collected, washed with physiological saline (NaCl 0.9%) and dried with filter paper. Brain samples were weighed and homogenized with a nine-fold aliquot of saline (NaCl 0.9%) under ice bath. Tissue homogenates were processed similarly as plasma samples. Plasma and tissue samples were frozen and stored at -80°C until analysis.

2.8. Assay of 3-HPA in plasma and brain tissue

HPLC-MS was used to analyze 3-HPA in samples. Briefly, 100 µL plasma samples (or 500 µL brain homogenate) of were transferred into 2 mL Eppendorf tubes. A volume of 200 µL (or 1 ml in case brain homogenate) of dichloromethane was added to each sample and mixed, using a vortex shaker (Neutec F202A0176 Model ZX3 Advanced Vortex Mixer, VELP Scientifica, Italy) at 4,000 rpm for 10 min. Then, the mixture was centrifuged (Eppendorf AG, Hamburg, Germany) for 6 min at 5,000 rpm to separate the layers. The lower organic layer was transferred to a flask and evaporated to dryness under a gentle stream of nitrogen. 3-HPA extraction procedure was repeated 2 times. The residue was then reconstituted with 1mL of dichloromethane, and centrifuged at 12,000 rpm for 5 min.

An aliquot (100 µL) of the clear supernatant was diluted in methanol and water (70:30, v/v). A system from the Agilent HPLC 1200 series (Agilent Technologies, USA) equipped with binary pump, vacuum degasser and autosampler was used to inject the samples. Aliquots of 10 µL were run using isocratic mobile phase consisting of methanol and water (70:30, v/v) pumped at a constant flow rate of 0.3 mL/min.

Quantitation was achieved by MS-MS detection in positive mode using AmazonX (Bruker Daltonik GmbH, Germany) mass spectrometer equipped with an electrospray ionization (ESI) source. The optimized operational parameters for MS analysis were −4500 V as the voltage on the capillary and 10 L/min the flux of nitrogen as a drying gas (250°C). Detection of ions was performed in the multiple reaction monitoring (MRM) mode, the transition pair of 3-HPA at the m/z 400 precursor ion to the m/z 382 product ion (Fig. 2).

The analytical data were processed using the Bruker Daltonics software. Calibration curves were acquired by plotting the peak area of the transition pair of analyte against the nominal

concentration of 3-HPA calibration standards in plasma (or brain homogenate). The concentrations used were 5, 10, 20, 50, 80 ng/mL. The calibration curve was linear over the concentration range of 5-100 ng/mL of 3-HPA in both rat plasma and in brain homogenate (Fig. 2d).

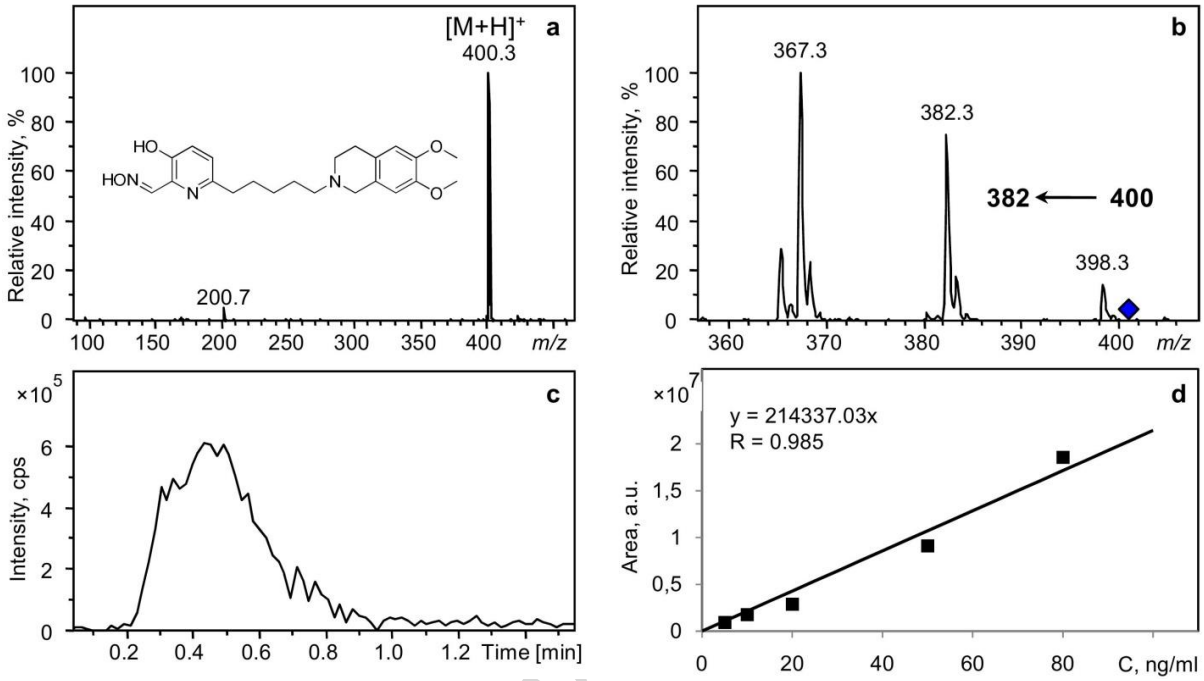

Fig. 2. Full scan mass (a) and product ion (b) mass spectra of 3-HPA in positive ionization mode. Typical MRM chromatogram of 3-HPA (c). Calibration curve of 3-HPA in brain homogenate (d).

2.9. Measurement of brain AChE inhibition and reactivation level

For brain AChE inhibition assays, rats were poisoned by 0.8×LD_{50} of POX (600 µg/kg, *i.p.*). Whole brains were collected 1 h, 6 hrs or 8 hrs after POX administration and frozen in liquid nitrogen. Whole brains of control group of rats were collected 1h after intraperitoneal (*i.p.*) injection of physiological saline. Thereafter, AChE activity of brain homogenates was analyzed. The mean brain AChE activity of poisoned animals (8 rats per group) was compared with mean brain AChE activity of control group (8 rats).

For *in vivo* brain AChE reactivation assay, 1 h after poisoning by 0.8×LD_{50} of POX, rats were *i.v.* injected (8 rats per each group) 3-HPA-loaded SLNs, 3-HPA solution (DMSO-water (50 w/w), 2-PAM water solution and 2-PAM+3-HPA-loaded SLNs at the same dose of 3-HPA (5 mg/kg) 2-PAM (5 mg/kg). Whole brains were then collected at different time intervals after administration of free 3-HPA or 2-PAM+HPA-SLNs or 3-HPA-SLNs and frozen in liquid nitrogen. The mean activity of brain AChE after injection of free 3-HPA or 3-HPA-loaded-SLNs

or free 2-PAM or 2-PAM+3-HPA-SLNs were compared to the mean brain AChE activity of poisoned group.

Whole brains homogenates were prepared in a Potter homogenizer with 0.05 M Tris-HCl, 1 % Triton X-100, 1 M NaCl, 2 mM EDTA; pH 7.0 (1 volume of brain for 2 volumes of buffer) at 4°C. The homogenates were centrifuged (10,000 rev/min, at 4ºC) for 10 minutes using Eppendorf 5430R centrifuge with FA-45-30-11 rotor (Eppendorf AG, Hamburg, Germany).

For AChE activity assay, 50µl supernatant was incubated with 5µl of tetra-isopropyl pyrophosphoramide (iso-OMPA) – as a butyrylcholinesterase specific irreversible inhibitor - in final concentration 0.1 mM, for 30 minutes. Then, AChE-catalyzed hydrolysis of substrate was started by adding of 10 µl of acetylthiocholine iodide (final concentration 1 mM). After 10, 20 or 30 min of hydrolysis at 25°C, reactions were stopped by adding the carbamylating agent neostigmine (0.1 mM). Samples were diluted in 50 mM phosphate buffer (pH 8.0) and DTNB (0.1 mM) was added. AChE activity was measured according to the Ellman method [23] by determining the production of yellow 5-thio-2-nitro-benzoate anion, resulting from reduction of DTNB by thiocholine (the product of substrate hydrolysis) at 412 nm by spectrophotometry (PerkinElmer λ25). The amount of thiocholine produced during 20 min (10th–30th min) was calculated. Sample without substrate was used as a blank. Three samples of each brain homogenate were measured independently. AChE activity was expressed in relation to the amount of total protein, which was determined by the Bradford method [24]. Data were analyzed using Origin 8 and expressed as the mean ± SEM. Two group comparisons were performed using Mann-Whitney test. $P < 0.05$ were considered statistically significant.

3. Results and discussion

3.1 Synthesis of 3-HPA

The synthesis of 3-HPA has been improved in comparison with those reported in [17]. The synthetic routes of 3-HPA are shown in Fig. 1. All the compounds were carefully purified and characterized by ^{1}H NMR and ^{13}C NMR. The synthesis started with the esterification of commercially available 3-hydroxypicolinique acid **1** followed by regioselective bromination of pyridine and finally benzylation of the 3-hydroxy function. Previous synthesis procedure of compound **4** was obtained with a non-optimized yield from 35 to 40 % (3 steps). Modification of the procedure allowed robust and easily upscalable production of **4** with 95% to quantitative yield, mainly by running the bromination step (c) at 0°C instead of room temperature, allowing a complete regioselectivity for the bromination reaction. Sonogashira cross-coupling reaction

leaded to the alcohol **5** with excellent yield (from 96 to 99%). Formation of the corresponding mesylate followed by a nucleophilic substitution with 6,7-dimethoxy-1,2,3,4-tetrahydroisoquinoline hydrochloride (TIQ.HCl) furnished the compound **6** with an acceptable yield of 74 % (63 % previously reported). Then concomitant reduction of the alkyne and deprotection of the phenol function was carried out using Pearlman's catalyst under a hydrogen atmosphere and MeOH as sole solvent to obtain compounds **7** quantitatively. Catalytic hydrogenation was then followed by a sequence of three reactions comprising (i) the protection of the phenol group with TBDMSOTf, (ii) the reduction of the methyl ester to aldehyde upon DIBAL-H treatment, and finally (iii) the deprotection of the TBDMS ether under the influence of TBAF. These transformations led to the aldehyde **8** in 67 % over three steps versus 11% over four steps previously reported, by changing the reaction conditions of protection step, adaptating the reduction step reaction time and equivalents of DIBALH, and performing the deprotection step at 0°C. The last step consisted of the formation of the oxime function with the condensation of hydroxylamine onto the aldehyde (76%). Altogether, the desired oxime has been obtained in eleven steps with 34-36% overall yield from **1** versus 5 % from **5** as previously reported.

3.2. Characterization of oxime-loaded lipid nanoparticles and study of in vitro oxime release

To prepare 3-HPA- loaded SLN and SLN with dual delivery of oximes (2-PAM and 3-HPA) we used the technique described earlier [13]. To characterize stability of oxime-loaded SLNs, particle sizes and zeta potential by dynamic light scattering during time were evaluated. Results are presented in Table 1 and Supplementary material (SM) (Fig. 3S, 4S).

The size of 3-HPA-SLNs is around 100 nm and it increased to 160 nm for dual delivery of 2-PAM+3-HPA-SLNs. Polydispersity index of 2-PAM-3-HPA-loaded SLNs is 0.61, it is higher than for empty SLNs (70 nm). The zeta potential of nanoparticles is reduced with increasing of the concentration of 3-HPA (Fig. 4S, SM) and in the case of dual delivery SLN. After 10-month storage at 4 ºC 3-HPA-SLNs and 2-PAM+3-HPA-SLNs showed a good stability. The size and polydispersity index did not change, the zeta potential slightly decreased. The encapsulation efficiency for 2-PAM is around 95%; and it is comparable with previous 2-PAM-loaded SLNs formulation. The encapsulation efficiency for 3-HPA of 3-HPA-SLNs and 2-PAM-3+HPA-SLNs formulations equals 52±2 % and 63.1±3%, respectively. The loading capacity is close to 4% for 3-HPA and 6% for 2-PAM.

Table 1.

Size (Hydrodynamic diameter), Polydispersity index (PdI), Zeta potential (ZP), encapsulation efficiency (EE, %), and loading capacity (LC, %) of nanoparticles (data are expressed as mean ± SD)

Formulation	1-day storage			10-month storage			EE, %		LC, %	
	Size, nm	PdI	ZP, mV	Size, nm	PdI	ZP, mV	2-PAM	3-HPA	2-PAM	3-HPA
Empty SLN	68±13	0.26±0.01	-55±1.5	-	-	-		-	-	
3-HPA-SLN	106±19	0.38±0.02	-30.0±0.7	106±19	0.39±0.1	-19.2±0.5	-	52±2		3.5±0.1
2-PAM+3-HPA-SLN	164±23	0.61±0.02	-25±5	106±16	0.49±0.2	-10.3±0.3	94.7±2	63.1±3	6.3±0.1	4.2±0.2

In vitro release of oximes was analyzed by HPLC-MS and spectrophotometry methods. As seen in Fig. 3A, the faster release of 2-PAM was observed for 2-PAM+3-HPA-loaded SLNs (Fig. 3A curve 2) compared to 2-PAM-loaded SLNs (Fig. 3A curve 1): 50% of 2-PAM was released in 10 minutes and 15 minutes (Fig. 3A curve 1), respectively.

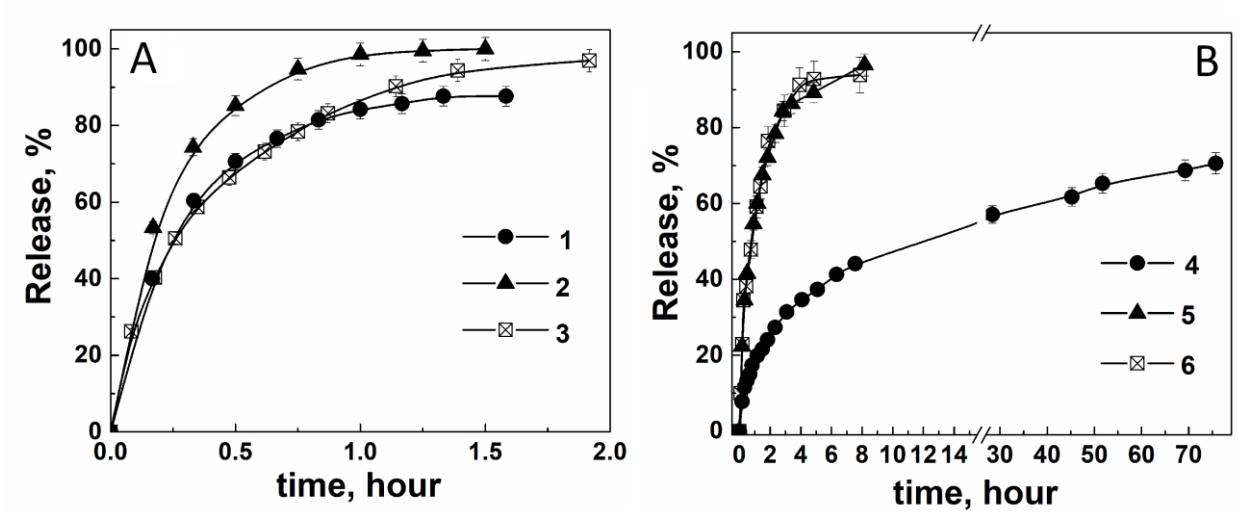

Fig. 3. *In vitro* release of 2-PAM (A) (1-3) and 3-HPA (B) (4, 5, 6) using the dialysis bag method (n =3) from 2-PAM-loaded SLNs (1); 2-PAM+3-HPA-loaded SLNs (2, 3, 6); 3-HPA-loaded SLNs (4, 5). The concentration of 2-PAM and 3-HPA is 0.1% (w/w). Phosphate buffer, 0.025 M (1, 2, 4), methanol-phosphate buffer (50% v/v) (3, 5, 6), pH = 7.4, 37 °C.

In vitro release time of 3-HPA was not dependent on the type of delivery formulation (Fig. 3B curves 5,6), i.e. 3-HPA-loaded SLNs versus 2-PAM+3-HPA-loaded SLN, but it was two orders slower than for 2-PAM: 50% of 3-HPA was released in 15 hours. The full release time of 3-HPA was more than 80 hours (Fig. 3B curve 4).

3.3. Pharmacokinetic study

The concentration of 3-HPA in plasma after one single intravenous injection of 3-HPA in DMSO-water solution (5 mg/kg) and loaded in SLNs with the same dose is shown in Fig. 4A.

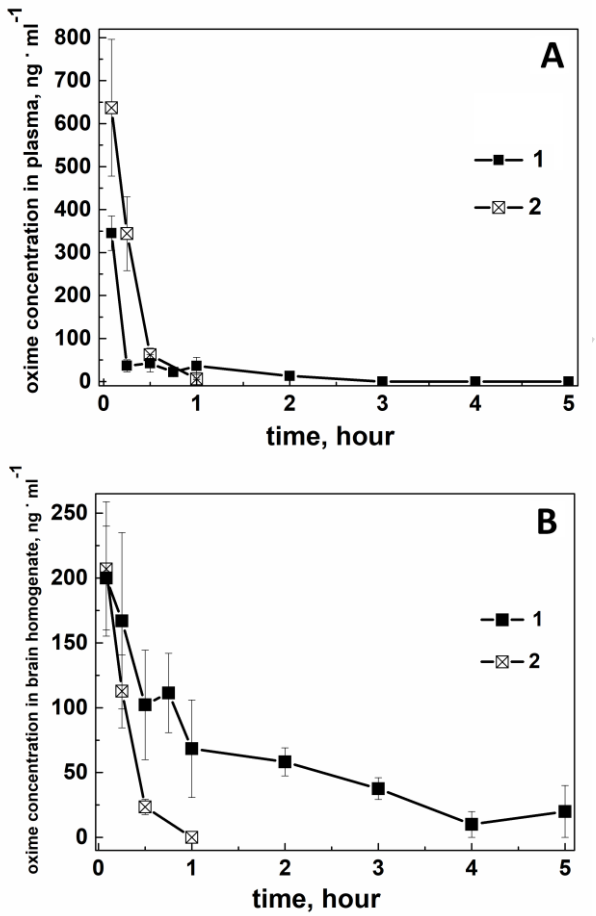

Fig. 4. Concentration of 3-HPA in rat plasma (A) and in rat brain homogenate (B) after intravenous injection of 3-HPA-loaded SLNs (1) free 3-HPA (2) in DMSO-water solutions (50% w/w). The dose of 3-HPA is 5 mg/kg for 3-HPAin DMSO-water solutions and 3-HPA-loaded-SLNs. Each point represents the mean ± SD in five rats.

The pharmacokinetics of 3-HPA in rat bloodstream can be described by a two-compartment model (3),

$$[C]_t = Ae^{-\alpha t} + Be^{-\beta t} \quad (3)$$

where $[C]_t$ is 3-HPA concentration in plasma at time t, α and β are distribution and elimination rate constants, respectively. The distribution phase α is very fast. Thus, we only monitored the elimination phase (β). At 5 min, the 3-HPA maximum concentration in plasma was 640 ng/ml; it progressively decreased to 6 ng/ml over 60 min.

Calculated pharmacokinetic parameters for elimination are summarized in Table 2. The elimination half-time ($t_{1/2\beta}$) for 3-HPA is 18 min, which is similar to elimination half-time of 2-

PAM ($t_{1/2\beta}$ = 24 min). The 3-HPA-loaded-SLNs exhibited an elimination half-time ($t_{1/2\beta}$) of 154 min, i.e. 8.5-fold longer than for free 3-HPA.

Table 2.

Pharmacokinetic parameters observed in rats after intravenous injection of 3-HPA in DMSO-water solutions (50% w/w), 3-HPA-loaded SLNs. The dose of 3-HPA is 5 mg/kg for 3-HPA in DMSO-water solutions (50% w/w) and in 3-HPA-SLNs preparation. Results represent the mean ± SE for five rats.

Samples	β, min^{-1}	$t_{1/2\beta}$*, min
3-HPA solution	0.03833±0.004	18±1
3-HPA-SLNs	0.00451±0.002	154 ±10

*$t_{1/2\beta}$= ln2/β, according to Eq.1 in which β is the elimination rate (min^{-1}) from blood.

To determine the ability of 3-HPA to cross the blood-brain barrier, 3-HPA in DMSO-water solution and 3-HPA-loaded SLNs were analyzed in brain tissues (Fig. 4B). It is clearly observed that the concentration of 3-HPA in the brain tissue in the case of 3-HPA-loaded SLNs is much higher than for injected free 3-HPA in DMSO-water solution.

3.4. Reactivation of Brain AChE in vivo

To test the *in vivo* reactivation of brain AChE, we used a rat model for OP toxicity using POX. One hour after poisoning by 0.8×LD_{50} of POX (600 µg/kg, *i.p.*), brain samples were collected and AChE activity was analyzed. One hour after administration of this sub-lethal dose of POX, the residual activity of brain AChE was 31±4% (Fig. 5, Fig. 6 dotted line). One hour after injection, the irreversible inhibitory action of POX on brain AChE reached a plateau, as evidenced by the level of AChE inhibition after one, six and eight hours (Fig. 5). Thus, recovery of AChE brain activity in the absence of AChE reactivators, due to possible *de novo* enzyme synthesis, was not significant ($p > 0.05$, Mann-Whitney test).

One hour after POX (600 µg/kg, *i.p.*), free 3-HPA (5 mg/kg) in DMSO-water solution (50% w/w), 3-HPA-loaded SLNs at the same dose (5 mg/kg), 2-PAM-loaded SLNs (5 mg/kg) and 2-PAM-3-HPA-loaded SLNs (5 mg/kg for 2-PAM and 5 mg/kg for 3-HPA) were injected. At different times after injection (0.5, 1, 3, 5 and 7 hours), brain samples were collected and activity of AChE was measured. We observed that after injection of free 3-HPA, phosphylated brain AChE was poorly reactivated: residual activity of brain AChE was about 34±3% and reactivation

was less than 5%. (Fig. 6, line 4). Likely, low brain AChE reactivation mediated by free 3-HPA is associated with its fast elimination rate (Fig. 4).

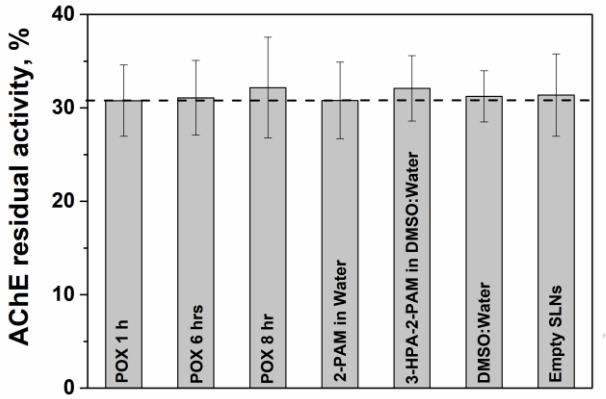

Fig. 5. Brain AChE activity 1h, 6 hrs, 8 hrs after poisoning of rats by POX (600 mg/kg, *i.p.*) and 7 hrs after *i.v.* injection of 2-PAM (5 mg/kg) in water, 3-HPA (5 mg/kg) in DMSO-water (50% w/w), DMSO-water (50% w/w) alone or empty SLNs to rats poisoned by POX (1 h, 600 mg/kg, *i.p.*). Mean AChE activity of brain homogenates measured in control group of rats was taken as 100%.

On the other hand, with 3-HPA-SLNs, 30% brain AChE reactivation is slowly achieved in 5 hours (Fig. 6, curve 1). After 7 hours the same level of reactivation was detected. It should be noted that this is the first example of high reactivation of phosphylated brain AChE. But there is a threshold (until 3 hours after 3-HPA-loaded SLNs injection) when brain AChE reactivation was only a few percent (Fig. 6). This could be attributed to possible *in vivo* very slow release of 3-HPA from SLNs (*in vitro* release takes more than 80 hours (Fig. 3B). The effect of 2-PAM-loaded SLNs (dose of 2-PAM 5 mg/kg) on brain AChE reactivation reached a plateau (15±3%) 1 hour after injection (Fig. 6 curve 2), i.e. the plateau appears earlier than for 3-HPA. Though the release of oximes from SLNs can be different *in vitro* and *in vivo*, *in vivo* reactivation kinetics of phosphylated brain AChE correlates with *in vitro* faster release time of 2-PAM from SLNs compared to release of 3-HPA (Fig. 3A). Therefore, it is assumed that the design of SLNs formulation for dual delivery of two oximes (2-PAM+3-HPA-loaded SLNs) with different release properties for both oximes makes it possible to increase the therapeutic time window for oximes. As we can see for combinational therapy with two SLN-encapsulated oximes, brain AChE reactivation takes place from 30 minutes to 7 hours and reaches 40±3% (Fig. 6 curve 3). This high reactivation level is clearly the result of the use of oxime nanoformulation, since injection of either free 2-PAM in water, 3-HPA in DMSO-water, only DMSO or empty SLNs

did not lead to significant increase in brain AChE reactivation of POX poisoned rats, 7 hours after injection of tested compounds (Fig. 5).

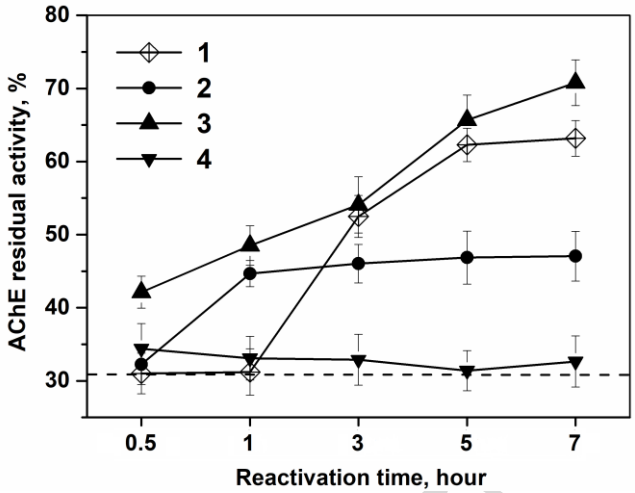

Fig. 6. Brain AChE reactivation level as a function of time after poisoning of rats by POX (600 mg/kg, *i.p.*) and subsequent *i.v.* injection 3-HPA-loaded SLNs (1), 2-PAM-loaded SLNs (2) or 2-PAM-3-HPA-loaded SLNs (3) and free 3-HPA in DMSO-water solution (4). Mean AChE activity of brain homogenates measured in control group of rats was taken as 100%. Data are expressed as mean ± SEM. The dotted line shows the level of residual brain AChE activity one hour after POX poisoning, without administration of reactivators.

It is important to note that 30 minutes after injection of 3-HPA-loaded SLNs or 2-PAM-loaded SLNs (dose 5 mg/kg of 2-PAM and 3-HPA, respectively), no reactivation of AChE was observed. Whereas injection of 2-PAM+3-HPA-loaded SLNs (dose of 2-PAM 5 mg/kg, 3-HPA 5 mg/kg) resulted in reactivation of 10% AChE activity (Fig. 6 curve 3 and Fig. 6S). Thus, in the initial part of reactivation curve an additive action of the two encapsulated oximes on phosphylated brain AChE is observed. It is important to note that for the other time points the additive effect of the two oximes is not observed. It also should be noted that the characteristics of oxime-loaded lipid nanoparticles (mean diameter around 100 nm and negative charge around −30 mV) are only slightly different between the two types of SLNs (single encapsulated oxime or two encapsulated oximes). Therefore, the additive action of oximes on AChE reactivation at 30 min-time point could be the result of *in vivo* alteration in the release time of 2-PAM and 3-HPA between single and double nano-formulations (cf. Fig. 3A for *in vitro* release). A possible interplay of both oximes on phosphylated AChE the 30 min-time point can also be considered. Given that the bimolecular rate constant of 3-HPA for POX-phosphylated AChE is higher than that of 2-PAM [17], an allosteric potentiation of 3-HPA-mediated reactivation of AChE by 2-

PAM may occur through binding of positively charged 2-PAM on the peripheral site of AChE. Further study should clarify this hypothesis.

The interactions between nanoparticles and biological environment in brain are complex and poorly known. There is little evidence that nanoparticles remain stable under conditions of the brain microenvironment [25]. The efficiency of delivery to the brain depends on numerous factors such as the ability of nanoparticles to move within the parenchyma [26], and the effective diffusion within the extracellular matrix [27]. In addition, it is well known that functionalization of SLNs can enhance brain drug delivery (uptake mechanism and transport pathways) [28]. The highest potential for brain delivery was found for SLNs stabilized by polysorbate 80 [29,30] and other poloxamers [31]. High delivery was also shown to be associated with difference in adsorption of apolipoprotein E (apoE) and BBB specific proteins on the surface of SLNs [29-32]. ApoE adsorbed on nanoparticles mediates their interaction with LDL (low density lipoproteins) or scavenger receptors located on the BBB. Then, brain uptake processes take place [33]. Protein crown bound on nanoparticles affects different processes of biological interest [34,35], including improvement of nanoparticle accumulation in the brain [36]. At the moment, we do not know either the mechanism of oxime-loaded SLNs transfer across the BBB or the release process of oximes. Further studies are needed to shed light on these mechanisms and to improve efficiency of brain AChE reactivation by optimizing nano-formulations. Special attention will be paid to characterization of the behavior and diffusive capability of nanoparticles as a function of their size, surface charge, surface coating under brain environment conditions.

4. Conclusions

In conclusion, several tasks were solved: i) encapsulation of 3-HPA in solid lipid nanoparticles increased the bioavailability (solubility) of 3-hydroxy-2-pyridine aldoxime (3-HPA) and prolonged circulation time in the bloodstream by 8.5 times compared to free 3-HPA; ii) 3-HPA-SLNs showed high reactivation of brain AChE (30%) inhibited by paraoxon; iii) overcoming BBB for 2-PAM and achieve sequential release of both oximes (2-PAM and 3-HPA) and prolongation of the time window of oxime therapy leading up to 35% brain AChE reactivation were reached. Further studies are needed to determine the mechanisms of crossing the BBB and *in vivo* release of oximes from SLNs. Also, it will be of paramount interest to determine whether SLNs association of 2-PAM and 3-HPA can reactivate *in vivo* tabun-inhibited AChE and AChE inhibited by other potent phosphoramidates [37,38].

Acknowledgements

Biochemical experiments was supported by the Russian Science Foundation, grant No. 14-50-00014 to Irina V. Zueva and Konstantin A. Petrov. This work was in part supported by the Direction Générale de l'Armement (through PhD Fellowship to Anissa Braïki), the Agence Nationale de la Recherche (ANR) (project ReCNS-AChE, grant number ANR-13-ASTR-0002-02) to Pierre-Yves Renard and Ludovic Jean. This work was also partially supported by INSA Rouen, Rouen-Normandie University, Centre National de la Recherche Scientifique (CNRS), Région Haute-Normandie (CRUNCh network), and the LabexSynOrg (ANR-11-LABX-0029) to Anissa Braïki, Pierre-Yves Renard and Ludovic Jean.

E. B. Souto acknowledges the financial support received from Portuguese Science and Technology Foundation (FCT/MCT) and from European Funds (PRODER/COMPETE) under the project references M-ERA-NET/0004/2015-PAIRED and UID/QUI/50006/2013, co-financed by FEDER, under the Partnership Agreement PT2020.

P. Masson was supported by the Russian Government Program of Competitive Growth of Kazan Federal University.

The authors gratefully acknowledge the CSF-SAC FRC KSC RAS for providing mass spectrometer access.

Author Contributions

Tatiana N. Pashirova developed preparation and characterization of SLN and performed *in vitro* drug release experiment; Irina V. Zueva and Konstantin A. Petrov performed biochemical experiments; Vasily M. Babaev and Ildar Kh. Rizvanov developed the technique of assay of 3-hydroxy-2-pyridine aldoxime in plasma and brain tissue by the HPLC-MS and analyze data obtained performed the experimental work on mass spectrometer equipped; Evgenia A. Burilova and Darya A. Samarkina performed extraction experiment for plasma and brain tissue; Anissa Braïki synthesized oxime 3-hydroxy-2-pyridine aldoxime and characterized properties of this oxime; Pierre-Yves Renard and and Ludovic Jean proposed the idea of synthesis of oxime 3-hydroxy-2-pyridine aldoxime and controlled it; Eliana B. Souto controlled the synthesis of SLNs; Lucia Ya. Zakharova proposed the idea of physico-chemical part of the work and controlled it; Patrick Masson designed experiments; Oleg G. Sinyashin proposed the idea of the whole work.

Conflict of interests

None

Abbreviations

AChE, acetylcholinesterase; BBB, blood brain barrier; OP, organophosphorus agent; BChE, butyrylcholinesterase; 2-PAM, Pralidoxime chloride; SLN, solid lipid nanoparticle; SNC, central nervous system.

Supplementary material. Supplementary data are available in the online version, at

References

[1] C.M. Hartshorn, M.S. Bradbury, G.M. Lanza, A.E. Nel, J. Rao, A.Z. Wang, U.B. Wiesner, L. Yang, P. Grodzinski, Nanotechnology strategies to advance outcomes in clinical cancer care, ACS Nano 12 (2018) 24-43. DOI:10.1021/acsnano.7b05108.

[2] W. Fan, B. Yung, P. Huang, X. Chen, Nanotechnology for multimodal synergistic cancer therapy, Chem. Rev. 117 (2017) 13566–13638. DOI:10.1021/acs.chemrev.7b00258.

[3] M. Huang, M. Hu, Q. Song, H. Song, J. Huang, X. Gu, X. Wang, J. Chen, T. Kang, X. Feng, D. Jiang, G. Zheng, H. Chen, X. Gao, GM1-modified lipoprotein-like nanoparticle: multifunctional nanoplatform for the combination therapy of Alzheimer's disease, ACS Nano 9 (2015) 10801-10816. DOI:10.1021/acsnano.5b03124.

[4] S. Gadde, Multi-drug delivery nanocarriers for combination therapy, Med. Chem. Commun. 6 (2015) 1916-1929. DOI: 10.1039/C5MD00365B.

[5] R.C. Gupta, Handbook of toxicology of chemical warfare agents, 2nd ed., Academic Press-Elsevier, Amsterdam, 2015.

[6] I. Mangas, E. Vilanova, J. Estevez, T.C.C. França, Neurotoxic effects associated with current uses of organophosphorus compounds, J. Braz. Chem. Soc. 27 (2016) 809-825.

[7] H. Thiermann, T. Zilker, F. Eyer, N. Felgenhauer, P. Eyer, F. Worek, Monitoring of neuromuscular transmission in organophosphate pesticide-poisoned patients, Toxicol. Lett. 191 (2009) 297-304. DOI:10.1016/j.toxlet.2009.09.013.

[8] L. Karalliedle, J. Henry, The acute cholinergic syndrome. In: L. Karalliedle, S. Feldman, J. Henrey, C.T. Marss (Eds): Organophosphates and Health, Imperial College Press, London, UK, 2001, 109-140,

[9] F. Worek, J. Jenner, H. Thiermann, Chemical warfare toxicology: management of poisoning; Royal Chemical Society, Abington, UK, 2016.

[10] P. Masson, Novel approaches in prophylaxis/pretreatment and treatment of organophosphorus poisoning, Phosphorus, Sulfur Silicon Relat. Elem. 191 (2016) 1433−1443. DOI:10.1080/10426507.2016.1211652.

[11] J.G. Clement, J.D. Shiloff, C. Gennings, Efficacy of a combination of acetylcholinesterase reactivators, HI-6 and obidoxime, against tabun and soman poisoning of mice. Arch Toxicol. 61 (1987) 70-75. DOI:10.1007/BF00324551.

[12] F. Worek, N. Aurbek, H. Thiermann, Reactivation of organophosphate-inhibited human AChE by combinations of obidoxime and HI 6 *in vitro*, J. Appl. Toxicol. 27 (2007) 582-588. DOI:10.1002/jat.1241.

[13] J. Kassa, K. Musilek, J.Z. Karasova, K. Kuca, J. Bajgar, Two possibilities how to increase the efficacy of antidotal treatment of nerve agent poisonings, Mini Rev. Med. Chem. 12 (2012) 24-34. DOI:10.2174/138955712798869011.

[14] S. Vilela, P. Salcedo-Abraira, I. Colinet, F. Salles, M. de Koning, M. Joosen, C. Serre, P. Horcajada, Nanometric MIL-125-NH2 metal–organic framework as a potential nerve agent antidote carrier, Nanomaterials 7 (2017) E321. DOI:10.3390/nano7100321

[15] J. Yang, L. Fan, F. Wang, Y. Luo, X. Sui, W. Li, X. Zhang, Y. Wang, Rapid-releasing of HI-6 via brain-targeted mesoporous silica nanoparticles for nerve agent detoxification, Nanoscale 8 (2016) 9537−9547. DOI:10.1039/C5NR06658A.

[16] T.N. Pashirova, I.V. Zueva, K.A. Petrov, V.M. Babaev, S.S. Lukashenko, I.K. Rizvanov, E. B. Souto, E.E. Nikolsky, L.Y. Zakharova, P. Masson, O.G. Sinyashin, Nanoparticle-delivered 2-PAM for rat brain protection against paraoxon central toxicity, ACS Appl. Mater. Interfaces. 9 (2017) 16922-16932. DOI:10.1021/acsami.7b04163.

[17] T. Zorbaz, A. Braïki, N. Maraković, J. Renou, E. de la Mora, N. Maček Hrvat, M. Katalinić, I. Silman, J.L. Sussman, G. Mercey, C. Gomez, R. Mougeot, B. Pérez, R. Baati, F. Nachon, M. Weik, L. Jean, Z. Kovarik, P.-Y. Renard, Potent 3-hydroxy-2-pyridine aldoxime reactivators of organophosphate-inhibited cholinesterases with predicted blood brain barrier penetration, Chem. Eur. J. 24(38) (2018) 9675-9691. DOI:10.1002/chem.201801394.

[18] R.H. Müller, U. Alexiev, P. Sinambela, C.M. Keck, Nanostructured lipid carriers (NLC): The second generation of solid lipid nanoparticles in ercutaneous penetration Enhancers, in: N. Dragicevic, H.I. Maibach (Eds.) Chemical methods in penetration enhancement: Nanocarriers, Springer, Berlin, 2016, pp. 161−185. DOI:10.1007/978-3-662-47862-2_11.

[19] S. Doktorovová, A.B. Kovačević, M.L. Garcia, E.B. Souto, Preclinical safety of solid lipid nanoparticles and nanostructured lipid carriers: current evidence from *in vitro* and *in vivo* evaluation, Eur. J. Pharm. Biopharm. 108 (2016) 235−252. DOI:10.1016/j.ejpb.2016.08.001.

[20] J.F. Fangueiro, T. Andreani, L. Fernandes, M.L. Garcia, M.A. Egea, A.M. Silva, E.B. Souto, Physicochemical characterization of epigallocatechin gallate lipid nanoparticles (EGCG-LNs) for ocular instillation, Colloids Surf. B Biointerfaces 123 (2014) 452−60. DOI:10.1016/j.colsurfb.2014.09.042.

[21] E.B. Souto, A.J. Almeida, R.H. Müller, Lipid nanoparticles (SLN®, NLC®) for cutaneous drug delivery: structure, protection & skin effects, J. Biomed. Nanotechnol. 3 (2007) 317-331. DOI: 10.1166/jbn.2007.049.

[22] K. Nebendahl, Routes of administration, in: The laboratory rat, G.J. Krinke (Ed.), Academic Press, London, 2000, pp. 463−483.

[23] G.L. Ellman, K.D. Courtney, V.Jr. Andres, R.M. Feather-Stone, A new and rapid colorimetric determination of acetylcholinesterase activity, Biochem. Pharmacol. 7 (1961) 88−95. DOI:10.1016/0006-2952(61)90145-9.

[24] M.M. Bradford, A Rapid and sensitive method for the quantitation of microgram quantities of protein utilizing the principle of protein-dye binding, Anal. Biochem. 72 (1976) 248−254. DOI:10.1016/0003-2697(76)90527-3.

[25] C. Curtis, D. Toghani, B. Wong, E. Nance, Colloidal stability as a determinant of nanoparticle behavior in the brain, Colloids Surf B Biointerfaces 170 (2018) 673-682. DOI: https://doi.org/10.1016/j.colsurfb.2018.06.050.

[26] E.A. Nance, G.F. Woodworth, K.A. Sailor, T.Y. Shih, Q. Xu, G. Swaminathan, D. Xiang, C. Eberhart, J. Hanes, A dense poly(ethylene glycol) coating improves penetration of large polymeric nanoparticles within brain tissue, Sci Transl Med. 2012, 4(149) 149ra119. DOI: DOI:10.1126/scitranslmed.3003594.

[27] P. Chaturbedy, M. Kumar, K. Salikolimi, S. Das, S.H. Sinha, S. Chatterjee, B.S. Suma, T.K. Kundu, M. Eswaramoorthy, Shape-directed compartmentalized delivery of a nanoparticle-

conjugated small-molecule activator of an epigenetic enzyme in the brain, J Control Release. 217 (2015) 151-159. DOI:10.1016/j.jconrel.2015.08.043.

[28] A.R. Neves, J.F. Queiroz, S.A.C. Lima, S. Reis, Apo E-functionalization of solid lipid nanoparticles enhances brain drug delivery: uptake mechanism and transport pathways, Bioconjug Chem. 28(4) (2017) 995-1004. DOI:10.1021/acs.bioconjchem.6b00705.

[29] A. Gessner, C. Olbrich, W. Schroder, O. Kayser, R.H. Muller, The role of plasma proteins in brain targeting: species dependent protein adsorption patterns on brain-specific lipid drug conjugate (LDC) nanoparticles, Int. J. Pharm. 214 (2001) 87-91. DOI:10.1016/S0378-5173(00)00639-6.

[30] T.M. Göppert, R.H. Müller, Polysorbate-stabilized solid lipid nanoparticles as colloidal carriers for intravenous targeting of drugs to the brain: Comparison of plasma protein adsorption patterns, J. Drug Targeting 13(3) (2005) 179–187. DOI: 10.1080/10611860500071292.

[31] T.M. Göppert, R.H. Müller, Protein adsorption patterns on poloxamer- and poloxamine-stabilized solid lipid nanoparticles (SLN), Eur. J. Pharm. Biopharm. 60(3) (2005) 361-372. DOI:10.1016/j.ejpb.2005.02.006.

[32] T.M. Göppert, R.H. Müller, Adsorption kinetics of plasma proteins on solid lipid nanoparticles for drug targeting, Int. J. Pharm. 302(1-2) (2005) 172-186. DOI: 10.1016/j.ijpharm.2005.06.025.

[33] J. Kreuter, Mechanism of polymeric nanoparticle-based drug transport across the blood-brain barrier (BBB), J. Microencapsul. 30(1) (2013) 49-54. DOI: 10.3109/02652048.2012.692491.

[34] J. Mo, Q. Xie, W. Wei, J. Zhao, Revealing the immune perturbation of black phosphorus nanomaterials to macrophages by understanding the protein corona, Nat. Commun. 9(1) 2018 2480. DOI:10.1038/s41467-018-04873-7.

[35] S. Schöttler, K. Landfester, V. Mailänder, Controlling the stealth effect of nanocarriers through understanding the protein corona, Angew. Chem. Int. Ed. Engl. 55(31) (2016) 8806-8815. DOI:10.1002/anie.201602233.

[36] R. Dal Magro, B. Albertini, S. Beretta, R. Rigolio, E. Donzelli, A. Chiorazzi, M. Ricci, P. Blasi, G. Sancini, Artificial apolipoprotein corona enables nanoparticle brain targeting, Nanomedicine. 14(2) (2018) 429-438. DOI:10.1016/j.nano.2017.11.008.

[37] S.E. Hosseini, H. Saeidian, A. Amozadeh, M.T. Naseri, M. Babri, Fragmentation pathways and structural characterization of organophosphorus compounds related to the chemical weapons convention by electron ionization and electrospray ionization tandem mass spectrometry, Rapid Commun. Mass Spectrom. 30 (2016) 2585–2593. DOI: 10.1002/rcm.7757.

[38] S. Costanzi, J.-H. Machado, M. Mitchell Nerve Agents: What they are, how they work, How to counter them, ACS Chem Neurosci. 19(5) (2018) 873-885, DOI:10.1021/acschemneuro.8b00148.

Graphical abstract